Research Article

Nano Biomed Eng

# Plant Ash/Polylactic Acid Electrospun Fiber Dressing Promotes Wound Healing Through pH Regulation

Yixuan Cai[1,2,§], Zhifeng Liao[3,4,§], Zhihao Xue[5,§], Zhaowen Xue[2], Jiayi Mei[6], Lin Zhou[2✉], Guojin Zhang[7✉], Wenyi Gan[1,2✉]

[1] Department of Traumatic Orthopedics, Zhuhai People's Hospital, Zhuhai 519050, China
[2] The First Affiliated Hospital of Jinan University, Guangzhou 510630, China
[3] Department of Plastic and Reconstructive Surgery, Guangdong Second Provincial General Hospital, Guangzhou 510310, China
[4] Plastic, Reconstructive and Hand Surgery Service, Lausanne University Hospital, University of Lausanne, CH-1011 Lausanne, Switzerland
[5] Department of Medicine, Jinan University, Guangzhou 510632, China
[6] Sun Yat-sen University Cancer Center, Guangzhou 510062, China
[7] PET Center, Department of Nuclear Medicine, Guangdong Provincial People's Hospital (Guangdong Academy of Medical Sciences), Southern Medical University, Guangzhou 510080, China

[§] These authors contributed equally to this work.

✉ Corresponding authors. E-mails: Wenyi Gan, 494414224@qq.com; Guojin Zhang, zhangguojin@gdph.org.cn; Lin Zhou, hyzhoulin@126.com

**Received:** Sep. 28, 2024; **Revised:** Dec. 7, 2024; **Accepted:** Dec. 27, 2024

**Citation:** Y.X. Cai, Z.F. Liao, Z.H. Xue, et al. Plant ash/polylactic acid electrospun fiber dressing promotes wound healing through pH regulation. *Nano Biomedicine and Engineering*, 2024, 16(4): 588−600.

http://doi.org/10.26599/NBE.2024.9290108

## Abstract

Wound healing has always been a focal point in medicine and fabrication of biomaterials. Nanofibers made from polylactic acid (PLA) promote wound healing and possess antibacterial properties. However, the acidic byproducts of PLA can hinder the wound-healing process. Plant ash, being mildly alkaline, has the potential to neutralize these acidic compounds. A nanofiber film combining PLA and plant ash can create a neutral environment conducive to cell growth. Additionally, the growth-promoting components of plant ash can further accelerate wound healing. In this study, we combined PLA with plant ash and electrospun the mixture into nanofibers, ultimately developing a pH-regulating wound dressing. We prepared a mixed emulsion containing grass and wood ash, PLA powder, and a polymer surfactant to fabricate the dressing. The emulsion was then frozen to reduce the solubility of the solvent, facilitating the precipitation of the plant ash/PLA mixture. Subsequently, nanofibers were produced from the precipitated powder through electrospinning, which were employed to create the wound dressing. We evaluated the degradation of the dressing in normal saline and monitored the pH changes over two weeks. The pH remained stable at 7–8, indicating a neutral to mildly alkaline state. This result confirms an optimal environment for wound healing.

**Keywords:** pH regulation; plant ash; wound healing; nanofibers

## Introduction

The skin plays an essential role as a protective layer that shields the internal organs from the external environment. Unintentional abrasions or injuries usually severely damage the skin and create wounds that are difficult to heal. When this protection is lost, exposure to environmental factors such as heat, dryness, and microbial infiltration can lead to

infections and other injuries [1,2]. Typically, acute or superficial wounds naturally heal within 12 weeks, whereas chronic ones may take longer than 3 months. If not treated properly, they can necessitate amputation or even lead to death [3]. Delayed wound healing can cause complications such as poor blood circulation, necrosis leading to gangrene, and other chronic infections at the wound site, ultimately leading to amputation. Therefore, wound healing is considered a significant topic in both basic research and clinical medicine. The problems posed by wounds seriously threaten the socioeconomic development of countries worldwide [4–6]. Skin wound healing is a complex physiological process. Ordinarily, it consists of four overlapping phases: hemostasis, inflammation, proliferation, and remodeling [7]. The pH of the skin environment plays a key role in the cellular/cell cycle processes throughout these four phases. As one of the fundamental parameters of the wound microenvironment, intra and extracellular pH markedly influences cellular (enzyme activity, macromolecule synthesis, and metabolite transport) and cell cycle processes (inflammation, collagen formation, and angiogenesis) in the four phases. Intact skin is naturally acidic, with a pH between 4 and 6 [8–10]. Due to microvascular leakage, the pH of the wound becomes more alkaline, usually 7.5–8.9, approaching the physiological pH (7.4) that favors bacterial infection, causing inflammation and prolonging healing [11–13]. When reestablishing the barrier function in chronic wounds, restoration of the acidic environment of the wound surface reduces the microbial load on the skin surface, decreases susceptibility to bacterial colonization, and also helps adipose tissue to resume metabolism; keratinocytes and fibroblasts tend to migrate to and proliferate in an alkaline environment with a pH of about 8.3 [11].

In this paper, inspired by the process of skin wound healing through pH change, we electrostatically loaded plant ash into PLA wound dressings utilizing the electrospinning drug loading technology. The electrostatic spinning technology is a convenient and effective method for producing ultrafine fibers [14]. Electrospun nanofibrous materials are ideal materials for fabricating skin tissue scaffolds due to their bionic structural features and good absorbency, biodegradability, aeration, hemostasis, and bacteriostasis, which can meet the requirements of different wound types. The electrostatic spinning drug-carrying technology enables the blending of drugs or bioactive compounds with polymer solutions and their transformation into fibers through the electrostatic spinning technology. It combines electrostatic spinning and drug carrier technologies, which can uniformly disperse drugs in nanofibers and form micro or nanoscale structures within them. This method is conducive to the controlled and sustained release of drugs and is being used increasingly.

We designed the PLA electrostatically spun wound dressing to regulate the pH value of the skin in the wounds at various stages to promote and accelerate wound healing. The electrostatically spun nanofibers serve as a carrier that maintains shape due to excellent mechanical strength during the early stage of wounding, provide a good physical barrier for wound healing, and lower the wound pH to as close as possible to the acidic environment of the naturally intact skin. During the period of reestablishing the barrier function of chronic wounds, the contact angle test indicated high hydrophilicity, making it suitable for application to wounds. Plant ash possesses anti-inflammatory and anti-diarrheal effects as described in the Compendium of Materia Medica (Ben Cao Gang Mu) [15] and is mainly used orally or externally. Plant ash, with its alkaline properties, can regulate the pH of the wound by neutralizing the lactic acid produced during PLA degradation. PLA electrospun wound dressings containing plant ash offer an effective strategy for designing wound healing materials. They are of great interest for wound management and staged recovery.

## Materials and Methods

### Materials

Polylactic acid (PLA, particle size: 3 mm, $M_w$: ~80,000) and 1,1,1,3,3,3-Hexafluoro-2-propanol (HFIP; 99.5%) were purchased from Shanghai Macklin Biochemical Co. Ltd., Shanghai, China. Plant ash ("Bai-Cao-Shuang" or "Fu-Qi-Mo" in Mandarin Chinese) was made in Anhui, China, and bought from Nanjing Tongrentang Health Pharmaceutical Group Co. Ltd., Nanjing, China. Fetal bovine serum (FBS), Dulbecco's Modified Eagle Medium (DMEM), phosphate-buffered brine (PBS, pH = 7.4), and other media were sourced from Solarbio Limited (Beijing, China). The rats were purchased from the Guangdong Medical Laboratory

Animal Center (Guangzhou, China). All other reagents utilized were of high purity and purchased from Macklin reagents (Shanghai, China).

## Preparation of the plant ash/PLA dressing

We prepared the plant ash/PLA dressing in two parts. In our pre-test, 10 mL of HFIP was used to dissolve (1 000 ± 50) mg of PLA or (200 ± 10) mg of PA with 800 mg of PLA. Then, 1 g of plant ash/PLA powder mixed in different proportions was put into 50 mL centrifuge tubes, and 10 mL of HFIP was added to each. Before adding the solvent, PLA was ground into a powder and mixed with plant ash. The mixing ratios of plant ash and PLA were 200:800 (mg) (plant ash/PLA 20:80), 150:850 (mg) (plant ash/PLA 15:85), and 100:900 (mg) (plant ash/PLA 10:90). After HFIP was added and stirred for 3 h, the solution was shaken evenly and was immediately placed in a refrigerator at −80 °C. At low temperatures, the solubility of HFIP decreased, the solute in the solvent precipitated, and formed ice crystals. After freezing the solution was squeezed to combine plant ash and PLA powder. After freezing for 2–3 days, the centrifuge tubes were removed and thawed to room temperature. Those without any precipitation were selected and the PA/PLA electrospun solution was obtained.

In the second part, the solution was placed into an electrospinning machine to prepare the nanofiber dressings. The applied voltage, flow rate, and collection distance were set at 25 kV, 1.2 mL/h, and 17.5 cm, respectively. The nanofibrous membranes obtained were vacuum-dried for 24 h to remove the residual solvent and labeled "PA/PLA n:n" according to the plant ash content. In addition, the simple PLA dressing was prepared from the 10% PLA solution and served as a control.

## Characterization of the plant ash/PLA dressing

### *Degradation performance and pH determination*

The natural wound healing process usually takes 14–21 days. The appropriate biodegradation cycles for biomaterials can benefit wound healing [16]. The PLA nanofiber and PA/PLA dressings were cut into pieces weighing (300 ± 3) mg and placed in normal saline containing 0.4% collagenase at 37 °C. The samples collected at different times for 14 days, were dried and weighed. The mass change was observed by taking the initial weight of the material as $W_1$ and the weight after degradation as $W_0$; the degradation rate was calculated by applying Eq. (1):

$$\text{Weight } mathrmloss\ (\%) = \frac{W_1 - W_0}{W_1} \times 100\% \quad (1)$$

Previous studies have indicated that the pH value also affects wound healing [11]. Wound healing requires a weakly acidic or neutral environment with a pH of 6–7 during the early stage and a weakly alkaline pH after day 7. We measured the pH value of the dressing surface with precision MQuant pH indicator test strips, pH 6.5–10.0 (Merck KGaA, Darmstadt, Germany) before drying the material for different times to evaluate whether the change in pH values due to the degradation of the material met the wound healing requirements.

### *Morphological analysis*

The samples were frozen in liquid $N_2$, cut into thin slices with a blade, placed on a copper platform, and sprayed with gold for observation. The surface morphology of the plant ash/PLA dressing was visualized using a Phenom G6 pro scanning electron microscope (SEM; Thermo Fischer Scientific, USA). The mean diameter of the fibers was measured utilizing the Image Pro Plus 6.0 software, and approximately 150 nanofibers per sample were analyzed.

### *FT-IR analysis*

The dressings were finely ground and mixed with KBr powder to obtain a homogeneous mixture, which was then pressed into a transparent thin sheet suitable for infrared analysis. The Fourier-transform infrared (FT-IR) spectra of the prepared transparent sheet were recorded employing an FT-IR spectrometer (Thermo Fisher Scientific, USA). The spectrum was measured at 4 000–500 $cm^{-1}$, with 64 scans for each sample to ensure a high signal–noise ratio and data reproducibility.

### *Water contact angle test*

The water contact angle of the samples containing water droplets of 2 μL was ascertained with a DSA100 contact angle goniometer (KRÜSS GmbH, Germany). In brief, water droplets were gently added to the sample surface via a microsyringe. A high-resolution camera captured and measured the dynamic contact angle between the droplet and the surface.

*Water absorption performance test*

Wound dressings must have good water absorption ability and maintain a moist microenvironment to aid wound healing [17]. The water absorption performance of the material was assessed per the method of Liu et al. [18]. The dried nanofiber film was cut to pieces about (500 ± 5) mg, weighed (recorded as $W_0$), and placed in a funnel containing filter paper to ensure that the whole sample could absorb water uniformly. Subsequently, phosphate buffer was slowly added to the funnel until the first drop of water fell from the bottom. Then, the wet sample was gently removed and weighed ($W_1$), and the absorption capacity was calculated employing Eq. (2):

$$\text{Water absorption capacity } (\%) = \frac{W_1 - W_0}{W_0} \times 100\% \quad (2)$$

*Mechanical performance test*

The mechanical properties of the plant ash/PLA dressing in the compression and tension modes were determined with an Instron 5543 universal testing instrument (Instron, USA). All dressings were made into 50 mm × 15 mm × 1 mm strips. The two ends were fixed to a tension meter, at which point the sample was exposed up to a length of 40 mm outside the clamp. After adjusting the parameters, the two ends were stretched in opposite directions at 0.1 mm/s to measure the tensile strength (Pa). Simultaneously, the change in length due to the mechanical stretching of the sample, i.e., the strain (%) was ascertained. The data collected were processed with the Bluehill Ver. 2 software, provided with the instrument.

*Cell viability studies*

The cytotoxicity of the PA/PLA dressing was evaluated using NIH-3T3 fibroblasts [19, 20]. The cells were incubated in 96-well plates at 1.5 × $10^4$ cells per well in a complete medium: DMEM, 10% FBS, 0.5% penicillin, and 0.5% streptomycin and incubated at 37 °C, 99.9% humidity, and 5% $CO_2$ (v/v). The old medium was removed after the cell morphology stabilized at 24 h of incubation, as observed with a light microscope. PA/PLA and PLA were thinly sliced to a diameter of (1.8 ± 0.1) mm, and the plant ash powder was placed in each of the three plates. Ash powder was placed in three 96-well plates, with three empty wells serving as the blank control group. The original culture medium was removed at 24, 48, and 72 h. Subsequently, 150 μL of the medium containing 10% CCK-8 reagent was added to each well, and incubated at 37 °C for 2 h. The $OD_{467}$ was measured with an enzyme meter. The absorbance was calculated per the Lambert–Beer law using Eq. (3) [16, 21, 22]:

$$A = \lg\frac{I_0}{I} = -\lg T \quad (3)$$

where $A$ is the absorbance, $T$ is the transmittance, $I_0$ is the incident light intensity, and $I$ is the transmitted light intensity.

The absorbance at day 1 was considered $A_0$, while that at 24, 48, and 72 h was taken as $A_1$. The cell proliferation rate was calculated by applying Eq. (4):

$$\text{Cell viability } (\%) = \frac{A_1}{A_0} \times 100\% \quad (4)$$

Furthermore, a live/dead cell staining kit was employed to quantify cell viability at 24, 48, and 72 h. PA/PLA, PLA, and plant ash powder were cut into 5-mm-diameter slices and placed in 24-well plates, with some empty wells as blank control groups. NIH-3T3 and HUVEC cells were used as model cell lines and were implanted into the wells of each group with a concentration of 1.5 × $10^4$ cells per well on average, and cultured in an incubator. Then the materials and medium were removed at 24 and 72 h. Next, 5 μL of calcein and 5 μL of pyridinium iodide were mixed with 20 mL of de-ionized sterile water and left to stand for 10 min to stabilize the cells in the dark. After 10 min of staining, the staining solution was removed, and the cells were washed with sterile water for 1 min. The cells were observed twice using a DMi8 S inverted fluorescence microscope (Leica, Germany).

*Animal studies*

To evaluate the skin repair and wound healing effects of the biomaterials, a mouse back skin wound model was used [23–25]. PA/PLA and PLA nanofiber membrane dressings were cut into sheets with 2 cm in thickness. Simultaneously, four groups of rats were anesthetized and their backs were shaved for skin preparation. Then, two wounds of 2 cm in dimaeter were made on the backs with sterilized surgical scissors after injecting local anesthetics. The above materials and plant ash powder, as a single group were applied to the wounds, and one group was reserved as a blank control. The changes in the wounds were observed from the day of modeling up

to 14 days, and tissue biopsies were taken on the final day. We further observed the pH dynamics of the tissue surface by placing a drop of PBS on the surface of the wounded tissue and testing it with pH paper. The embedded tissues and sections were stained by hematoxylin and eosin (H&E), Masson trichrome, and immunofluorescent staining of CD31 and CD68 to analyze the effects of the materials on wound healing.

*RNA extraction and qRT-PCR analysis*

The impact of materials on skin repair can be assessed by detecting the cytokines expressed by macrophages [26, 27]. RAW264.7 macrophages in their logarithmic growth phase were cultured in Petri dishes. After the cells had fully adhered to the walls, 1 μg/mL of lipopolysaccharide (LPS) was added and incubated for 12 h. This differentiated the cells from the $M_0$ to the $M_1$ phenotype. The M1 phase macrophages were then inoculated into 6-well plates at $2 \times 10^5$ cells per well. PA/PLA dressings (pH = 8), PLA dressings (pH = 8), PLA dressings (pH = 7), and plant ash powder (pH = 9) were added after presoaking in deionized water for 7 days; a blank control group was set up. After 48 h of coincubation, the total RNA was extracted utilizing TRIzol (Thermo Scientific, MA, USA). The sample was quantified on an ND-1000 spectrophotometer (Nanodrop Technologies, DE, USA). RNA was reverse transcribed into cDNA employing the RevertAid First Strand cDNA Synthesis Kit (Thermo Scientific) following the manufacturer's instructions. The reaction mixtures (20 μL) were incubated in a PowerUp SYBR thermal cycler (Applied Biosystems, Germany) for 5 min at 25 °C, 20 min at 46 °C, 1 min at 95 °C, and then maintained at 4 °C. The mixtures were added with PowerUp SYBR ®Green Master Mix (Applied Biosystems, Germany), and the Step One Plus RT-PCR system (Applied Biosystems, Germany) was used for qRT-PCR. The expression levels were calculated using the relative $2^{-\Delta\Delta C_T}$ quantification method. All factors detected in the results were expressed as $C_T$ values. The $2^{-\Delta\Delta C_T}$ results were calculated using β-actin as an internal control. The multiplicity of expression in the blank control group and the test samples were calculated using Eq. (5) [28,29]:

$$2^{-\Delta\Delta C_{T_{Sample}}} = 2^{-(C_{T_{Sample}} - C_{T_{Reference}}) - (C_{T_{Control}} - C_{T_{Reference}})} \quad (5)$$

The primer sequences used for qRT-PCR analysis are shown in Table 1 [28].

*Statistical analysis*

All the quantified data were represented as the mean (± SD) and a $p$ value of $< 0.05$ was considered statistically significant, which was evaluated by applying the Student's Test and one-way ANOVA. All experiments were carried out in at least three independent replications. In addition, SPSS v.13.0.0 (IBM, NY, USA) was employed for the statistical analyses, and the quantitative fluorescence analysis of the photographs was performed by Image Pro Plus 6.0 (https://mediacy.com/image-pro/).

# Results and Discussion

## Characterization of the dressings

*Biodegradability and pH variation*

Biomaterials usually require improved degradability. In this regard, PLA is non-toxic, harmless, and degradable, thereby attracting much attention in the academic community in recent years [30–32]. We found that the degradation of the PLA nanofibers was slightly faster than that of PLA particles. As finer fibers increase the surface area of the material, more area contacts with water, which makes the material degrade faster. The PA/PLA composite fibers degraded marginally more rapidly than the PLA fibers alone; we deduced that the release of the plant ash in the material fibers caused them to lose weight (Fig. 1(a)). In several sets of nanofiber membranes with different PA/PLA ratios, the ratio of plant ash to PLA did not remarkably affect the degradation rate.

The degradation rate of the PLA materials was generally slow during the first four days because the materials did not start to degrade sufficiently, the plant ash in the materials was not released, and the surface pH of the materials immersed in the liquid was neutral (pH: 7–7.5). The PLA nanofibers gradually degraded from the early pH of 7 to a slightly acidic environment of pH = 6 in 14 days, whereas the plant ash powder solution always maintained an alkaline environment (pH: 9–10). According to previous reports, these conditions are unfavorable for wound healing [11]. PA/PLA at 20:80 remained neutral or weakly base for 14 days (pH = 7.5–8.5), and PA/PLA 10:90 maintained a neutral pH (7–7.5) in early days and showed a weakly alkaline

**Table 1** Forward (F) and reverse (R) primer sequences used in qRT-PCR analysis.

| Gene | Primer sequences (5'→3') |
|---|---|
| *β-actin* | F: ACCCAGATCATGTTTGAGACC |
| | R: GATCTTCATGAGGTAGTCTGTC |
| *TGF-β2* | F: CCGTTGTTCAGCCACTCT |
| | R: ATCCCGCCCACTTTCTAC |
| *Collagen I* | F: ACATGCCGTGACCTCAAGAT |
| | R: ATGTCC ATTCCGAATTCCTG |
| *Collagen III* | F: CTGGACCTGTTGGTCCATCT |
| | R: ATGCCATTAGAGCCACGTTC |

pH (7.5–8) from 12 days onward (Figure 1. B, Table 2). PA/PLA 15:85 could provide a weakly acidic microenvironment with a pH value of 7–7.5, a subsequent rise in pH to neutral conditions or weakly alkaline (pH: 7.5–8.5) during days 6–8, and tenable weakly alkaline from pH 8 to 8.5 after day 10.

In short, through the degradation patterns of PLA, we found a suitable content of plant ash and PLA: 150 mg plant ash and 850 mg PLA in 10 mL HFIP; PA/PLA 15:85. This combination rendered the material weakly acid in the early stage of wound healing, reducing the risk of bacterial infiltration; and in the middle and late stages, the weakly alkaline plant-ash particles (pH = 9) were released to properly neutralize the weakly acidic PLA nanofibers (pH = 6), so that the material surface created an environment suitable for the wound healing in the mid–late-stages, maintaining a pH range of 7.5–8 (Fig. 1(b), Table 2). Because PA/PLA 15:85 was able to synchronize with the pH changes required for skin repair, we used it for subsequent characterization experiments as well as for application in the animal wound models.

### *Fiber morphology*

PLA nanofibers obtained from electrostatic spinning had average diameters of 140–240 nm (Fig. 1(c)); PA/PLA fibers had diameters about 220–320 nm (Figure 1. D). The nanofibers obtained from electrostatic spinning provide a good environment for cell adhesion [33]. PLA nanofibers were arranged at an angle of 30°–60°, and after loading the plant ash, was 60°–90°, which was favorable for cell growth. The nanoscale pores between the materials allow breathing and block bacterial invasion [34–36].

### *FT-IR spectroscopy*

The FT-IR spectra of the product confirmed the occurrence of grafting (Fig. 2(a)). After loading plant ash, the O–H stretching vibration peaks at 3 200–3 500 $cm^{-1}$ while the O=C–O antisymmetric and symmetric stretching vibration peaks at 1 500–1 700 $cm^{-1}$ disappeared, indicating that the plant ash was successfully grafted onto the PLA. The C–H

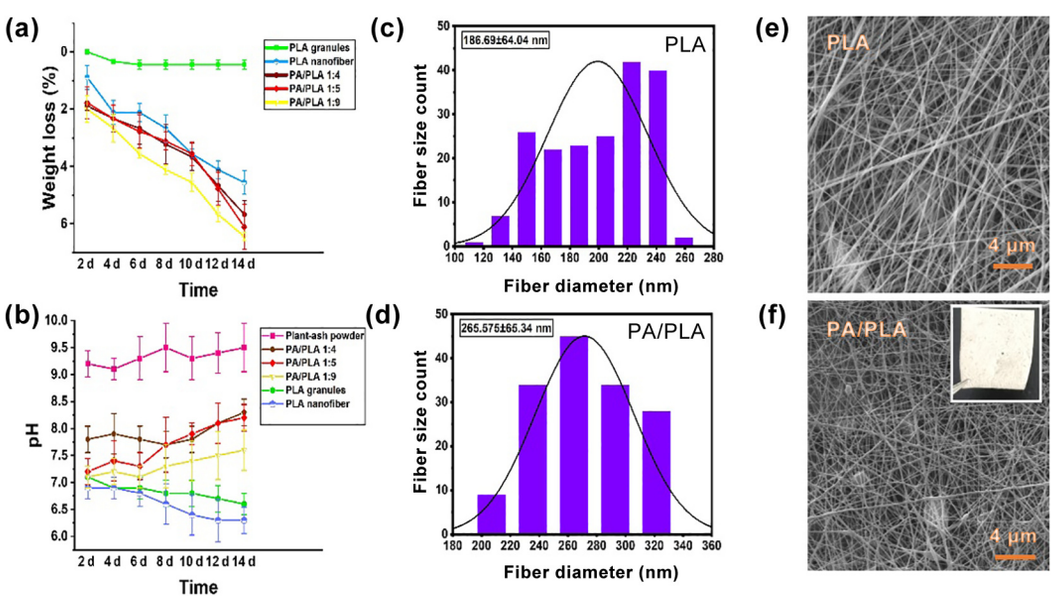


**Fig. 1** Degradation of several dressings, the resulting pH changes, and their microstructural characteristics. **(a)** The mass loss rate of PLA particles, PLA nanofibers, and PA/PLA nanofibers post-degradation; **(b)** pH changes on the surfaces of the degraded PLA particles, PLA nanofibers, and PA/PLA nanofibers; **(c)** Fiber diameter distribution of the PLA nanofibers; **(d)** Fiber diameter distribution of the PA/PLA nanofibers; **(e)** SEM observation graph of the PLA nanofibers; **(f)** SEM observation graph of the PA/PLA nanofibers.

**Table 2** The average of the pH change values of the surfaces of the degraded PLA particles, PLA nanofibers, PA/PLA nanofibers, and PA powder.

| | 2 days | 4 days | 6 days | 8 days | 10 days | 12 days | 14 days |
|---|---|---|---|---|---|---|---|
| **PLA particles** | 7.1 | 6.9 | 6.9 | 6.8 | 6.9 | 6.8 | 6.5 |
| **PLA nanofiber** | 6.9 | 6.9 | 6.8 | 6.6 | 6.4 | 6.3 | 6.3 |
| **PA/PLA 20:80** | 7.8 | 7.9 | 7.8 | 7.7 | 7.8 | 8.1 | 8.3 |
| **PA/PLA 15:85** | 7.2 | 7.4 | 7.3 | 7.7 | 7.9 | 8.1 | 8.2 |
| **PA/PLA 10:90** | 7.1 | 7.2 | 7.1 | 7.3 | 7.4 | 7.5 | 7.6 |
| **Plant-ash powder** | 9.2 | 9.1 | 9.3 | 9.5 | 9.3 | 9.4 | 9.5 |

stretching vibration peaks at 2 800–3 000 $cm^{-1}$ were also altered. In addition to the peaks of PLA itself ($–CH_3$ and –CH), $–CH_2$ peaks were also identified in the plant ash. Finally, a comparison of the bending vibration peaks of C–H at 1 300–1 400 $cm^{-1}$, suggested that the peaks after loading plant ash were larger in area and had more C–H bonds. The above comparisons illustrate the successful loading of plant ash by PLA.

*Wettability*

The contact angles of the nanofiber dressings indicated that the hydrophilicity of the simple PLA material was average, and more than 2 min elapsed from the time a water droplet hit the material surface to the time it was absorbed. The contact angle of the PA/PLA nanofibers decreased instantly from 72.2° to 0° in 8 s (Fig. 2(b)), indicating the extreme hydrophilicity and moisture retention of the material.

*Water absorption performance*

In comparison with the PLA nanofibers alone, the water absorption rate of the nanofibers loaded with plant ash was higher; the more the percentage of plant ash, the greater the water absorption (Fig. 2(c)). PA/PLA could absorb about 36% of its water mass, which was about 15% higher than that of the PLA dressings. While plant ash structurally changes the PLA nanofibers, it also significantly impacts water absorption. A moist environment is conducive to wound healing [16, 37], as it is conducive to cell recruitment to the wound, leading to the proliferation of granulation tissue. PA/PLA dressings fit this profile while promising aid in wound healing.

*Mechanical properties*

The application of biomaterials to human skin requires at least 2 MPa of mechanical strength [38]. PLA has good mechanical properties; in this study, the PLA and PA/PLA material had about 8 MPa of mechanical strength. The PA/PLA dressing can produce about 13.8% of the strain under mechanical tension after loading, which is in line with the biomechanical requirements of human skin (Fig. 2(d)).

## *In vitro* biocompatibility assessment

The viability of NIH/3T3 cells was measured at 24, 48, and 72 h to assess the effects of the different dressings on cell proliferation (Fig. 3(a)). The addition of the PA/PLA dressings did not affect cell proliferation, and the cell value-added rate of the PA/PLA co-culture was slightly higher than that of the PLA cell co-culture. In addition, the live/dead staining results indicated that the activity of both cell types increased after co-culture with PA/PLA (Figs. 3(b) and 3(c)), and the morphology of the PA/PLA cocultured cells was better than that of the other groups. The environment also affected cell growth (Figs. 3(d) and 3(e)).

## Effect of nanofiber scaffolds on the rat wound model

Wound modeling was performed on the back of the rats, and the wound repair process was observed (Fig. 4(a)). The repair effect of PA/PLA was markedly better than that of the other groups (Fig. 4(b)), and the wound area of PA/PLA and PLA was significantly smaller than that of the PA and blank control groups after 5 days. The physical barrier of the electrostatic spinning dressings helped isolate airborne microorganisms [39–41], a property that helped wound tissue regeneration in this experiment.

We simultaneously tested the pH of the skin tissue surface at each observation time and recorded its average value. The changes in the pH of the tissue surface were neutral at the beginning of wound creation; the wounds in the blank control group

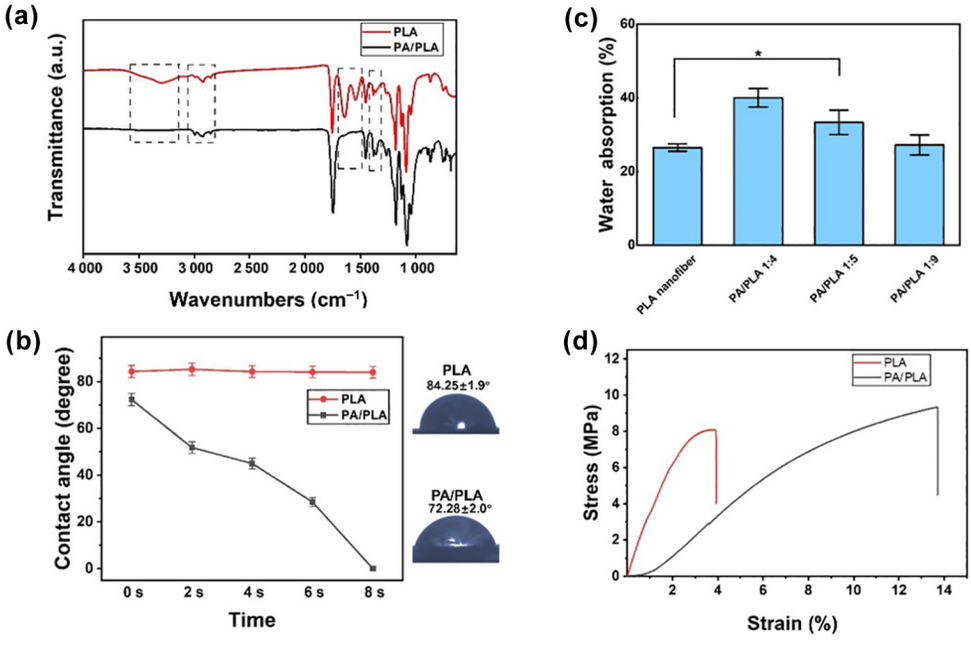


**Fig. 2** Characterization of PLA and PA/PLA nanofiber dressings. **(a)** FT-IR absorption peaks of PLA and PA/PLA; **(b)** Contact angles of PLA and PA/PLA; **(c)** Absorptive swelling rates of PLA and PA/PLA; **(d)** Mechanical tensile curves of PLA and PA/PLA; * $p < 0.05$.

indicated that natural wounds have always been weakly alkaline or neutral (Fig. 4(a)), These results are the same as that previously reported in the literature [11], and this environment may not be conducive to tissue makeover and contributes to the growth of pathogens such as bacteria that can cause infections. The pH changes in the experimental group with the electrostatically spun nanofiber dressing were similar to the values obtained in our previous experiments. PLA nanofibers alone make the wound consistently acidic, which can be detrimental to the growth of cells in the wound in the second week of skin repair. In contrast, the rats treated with plant ash alone (the PA group), consistently showed alkaline conditions, which in the first week, when the skin may be most susceptible to infection, deprives it of the naturally required acidic immune barrier or possibly helps pathogens grow in the wounds. In contrast, the composite PA/PLA nanofibers allowed the skin to maintain a relatively neutral environment early on, which combined with the physical barrier of its electrostatic spinning process, ensured that the skin tissues were protected from pathogens, and in the second week, because of the release of plant ash, began to present a weak alkaline condition. This effect per previous reports, facilitated the provision of nutrients to the fibroblasts by the surrounding cells and promoted skin tissue remodeling.

The tissue pH in the PA group declined on day 10 and became neutral on the last day of the experiment, which may be related to the degradation of the material.

## Histopathological analysis

We performed pathological and histological observations of the wound tissues of each group on day 14. H&E staining revealed the histopathological changes on day 14 of trauma (Fig. 5(a)). PA/PLA and PLA healed better and the repair was significantly higher than the blank control group. The wound healing in the plant ash group was marginally slower than that in PA/PLA and PLA due to the absence of the physical barrier formed by electrostatically spun nanofibers; the wound scabs remained, with obvious inflammatory cell infiltration. PLA wound contraction was apparent, and no wound was seen in the epidermis; but there were still a large number of inflammatory cells and less neovascularization. PA/PLA had remarkably more neovascularization than the other three groups due to plant ash loading which can regulate the wound pH, i.e., a good ability to produce blood vessels. The surface wounds of the PA/PLA group were no longer free of blood scabs, the inflammatory cells were reduced, and the inflammation had almost disappeared, with cuticle and new hair follicle formation, indicating the late stage of wound healing.

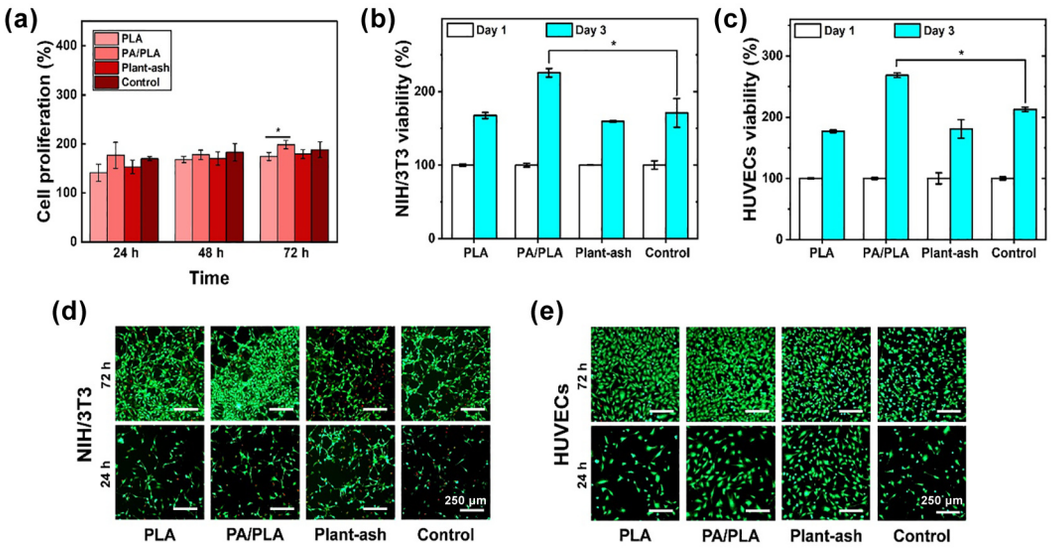


**Fig. 3** Biocompatibility of the nanofiber dressing **(a)**; cell proliferation of NIH/3T3 determined by CCK-8 assay at 24, 48, and 72 h; two kinds of fluorescence quantification after the live staining of NIH/3T3 **(b)** and HUVECs **(c)** cells. Cell viability of NIH/3T3 **(d)** and HUVECs **(e)** ascertained by live/dead staining on Day 1 and 3; *$p < 0.05$.

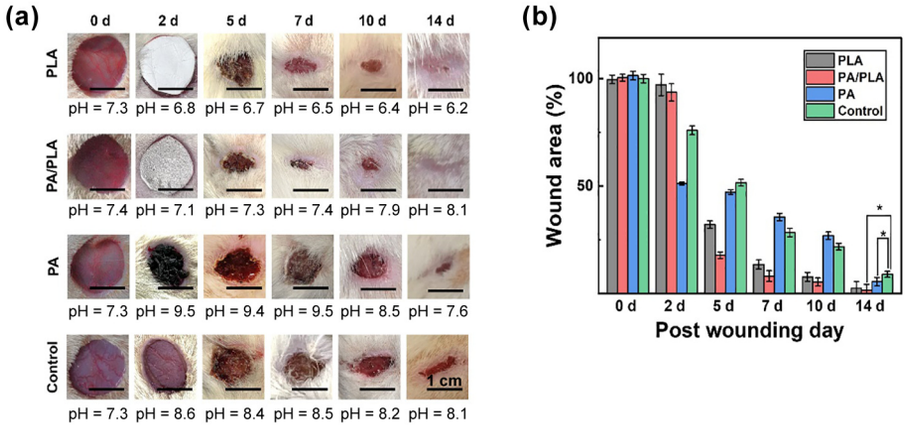


**Fig. 4** *In vivo* evaluation of wound healing in SD rats. **(a)** Photograph of wounds treated with blank (control), PLA, PA/PLA, and plant ash. **(b)** Wound closure rate at different times; *$p$ <0.05.

Collagen deposition serves as a critical biomarker for assessing the effectiveness of wound healing [42], as it reflects the structural integrity and functional recovery of the regenerated tissue. The density and arrangement of collagen fibers in neonatal skin tissues at varying stages of treatment were evaluated employing Masson trichrome staining, which highlights collagen deposition in blue (Fig. 5(b)). The results demonstrated a significant increase in collagen density under the influence of the electrospun nanofiber dressings. Among the tested groups, the PA/PLA dressings exhibited superior performance compared to the other materials, indicating their enhanced ability to support extracellular matrix formation and tissue remodeling during the healing process.

In addition to collagen deposition, neovascularization plays an essential role in wound repair by supplying $O_2$ and nutrients to the regenerating tissue. CD31, a vascular endothelial cell marker, is commonly utilized to evaluate angiogenesis during wound healing. Immunofluorescence staining demonstrated CD31 protein expression across all experimental groups [16, 42]. However, the control group exhibited markedly reduced levels of CD31 compared with the treated groups, with the PA/PLA group showing the highest expression (Fig. 5(c)). This finding underscores the critical role of PA/PLA dressings in promoting vascular regeneration, suggesting that the composite nanofiber dressing not only facilitated tissue repair but also enhanced the formation of

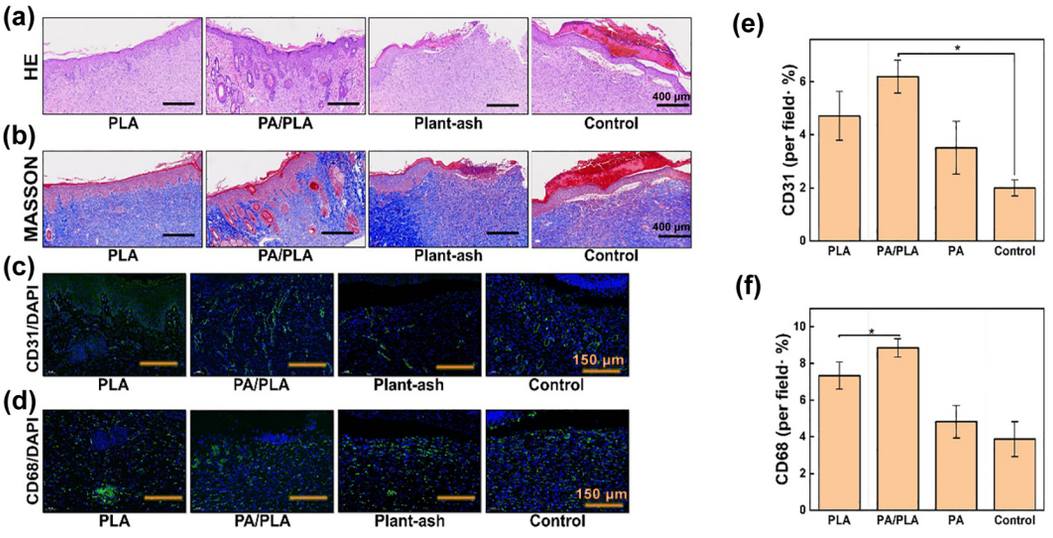


**Fig. 5** Histological analysis of re-epithelialization formation, collagen deposition, and angiogenesis in the wounds of different groups. **(a)** H&E staining and **(b)** Masson's trichrome staining images of the wound samples on day 14. Immunofluorescence detection of CD31 **(c)** and CD68 **(d)**; Quantitative analysis of CD31 **(e)** and CD68 **(f)**; *$p < 0.05$.

functional blood vessels necessary for sustained healing.

Macrophages are pivotal to wound healing, playing diverse roles in the inflammatory and tissue repair phases. They contribute to pathogen clearance, granulation tissue formation, and the secretion of cytokines and growth factors that regulate the healing process. CD68 is a marker of macrophage activity [42] and is employed to evaluate immune response and macrophage recruitment within the wound site. On day 14 post-treatment, CD68 expression in the PA/PLA group was remarkably greater than that in the control group (Fig. 5(d)). This increase indicates enhanced macrophage activity, which is critical for both the resolution of inflammation and the transition to tissue regeneration. Quantitative immunofluorescence analysis confirmed that the PA/PLA-treated wounds exhibited a more than 2-fold enhancement in both CD31 and CD68 expression compared with the control group (Figs. 5(e) and 5(f)).

These findings highlight the benefits of PA/PLA dressings in creating a microenvironment that is highly conducive to efficient wound healing. The synergy between enhanced collagen deposition, increased vascularization, and macrophage-mediated repair demonstrates the potential of PA/PLA electrospun nanofibers as an advanced wound care material with broad therapeutic applications.

## Gene expression analysis

In previous studies, we found that *TGF-β2* is involved in the macrophage inhibition of inflammation and that *Collagen I* and *Collagen III* suggest subcutaneous connective tissue regeneration [28, 29]. We analyzed the expression levels of these three genes and found that PA/PLA was superior and statistically more significant to PLA in terms of *TGF-β2* and *Collagen I* expression (Figs. 6(a) and 6(b)) and to the plant ash added group in terms of *Collagen III* expression (Fig. 6(c)). Overall, the PA/PLA group had higher

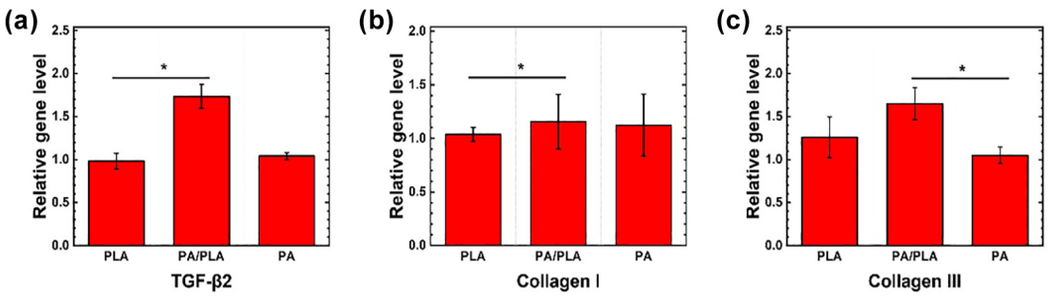


**Fig. 6** Effects of PLA, PA/PLA, PA on *TGF-β2* **(a)**, *Collagen I* **(b)**, and *Collagen III* **(c)** expression by RAW264.7 cells. Results are normalized to the endogenous control β-actin and presented as the fold change in expression levels relative to RAW264.7 on day 0. Values are expressed as the mean ± SD ($N = 3$); *$p < 0.05$.

healing indicators than the other groups.

## Conclusions

We developed an innovative electrospun dressing that combines the unique properties of PLA electrospun fibers and plant ash, leveraging their complementary characteristics to create a cutting-edge solution for wound healing. By ingeniously utilizing the pH-responsive attributes and modulating the plant ash loading ratio, we engineered a nanofiber dressing capable of providing an adaptive environment that optimally supports the wound-healing process. This advanced dressing exhibits a stable fiber structure, offering a robust physical barrier against bacterial invasion. Its inherent hydrophilicity ensures a clean and moist microenvironment conducive to tissue regeneration. Furthermore, the material has been validated for biosafety and demonstrates the ability to stimulate the proliferation of fibroblasts and vascular endothelial cells, which are key players in tissue repair. The dressing proved its therapeutic efficacy in animal wound modeling experiments by promoting macrophage recruitment, facilitating collagen network reconstruction, and enhancing vascular regeneration. These effects are mediated by the regulated expression of critical genes, including *TGF-β2*, *Collagen I*, and *Collagen III*, as well as the suppression of excessive inflammation. Such findings highlight the dressing's potential to accelerate the healing process while mitigating inflammatory responses.

Our research underscores the significant promise of pH-regulated electrospun dressings in advancing wound care. Beyond their immediate applications, these dressings represent a harmonious integration of traditional Chinese medicine principles and state-of-the-art electrospinning technology. This innovative approach paves the way for new possibilities in wound management and the broader field of biomedical materials.

## CRediT Author Statement

**Yixuan Cai:** methodology, investigation, software, and writing original draft. **Zhifeng Liao:** formal analysis, methodology, and data curation. **Zhihao Xue:** methodology and validation. **Zhaowen Xue:** visualization and data curation. **Jiayi Mei:** visualization and data curation. **Lin Zhou:** conceptualization and validation. **Guojin Zhang:** writing–review, editing, conceptualization, and supervision. **Wenyi Gan:** conceptualization and supervision.

## Acknowledgements

This work was supported by the Guangzhou Municipal Science and Technology Program (No. 202102080400).

## Conflict of Interests

The authors declare that no competing interest exists.

## References

[1] N. Wang, B. Hong, Y.C. Zhao, et al. Dopamine-grafted oxidized hyaluronic acid/gelatin/cordycepin nanofiber membranes modulate the TLR4/NF-kB signaling pathway to promote diabetic wound healing. *International Journal of Biological Macromolecules*, 2024, 262: 130079. https://doi.org/10.1016/j.ijbiomac.2024.130079

[2] X.L. Yang, J.C. Yang, L. Wang, et al. Pharmaceutical intermediate-modified gold nanoparticles: Against multidrug-resistant bacteria and wound-healing application *via* an electrospun scaffold. *ACS Nano*, 2017, 11(6): 5737−5745. https://doi.org/10.1021/acsnano.7b01240

[3] E.M. Tottoli, R. Dorati, I. Genta, et al. Skin wound healing process and new emerging technologies for skin wound care and regeneration. *Pharmaceutics*, 2020, 12(8): 735. https://doi.org/10.3390/pharmaceutics12080735

[4] L. Shi, X. Liu, W. Wang, et al. A self-pumping dressing for draining excessive biofluid around wounds. *Advanced Materials*, 2019, 31(5): e1804187. https://doi.org/10.1002/adma.201804187

[5] E.B. Yahya, M.M. Alzalouk, K.A. Alfallous, et al. Antibacterial cellulose-based aerogels for wound healing application: A review. *Biomedical Research and Therapy*, 2020, 7(10): 4032−4040. https://doi.org/10.15419/bmrat.v7i10.637

[6] R. Tarrahi, A. Khataee, A. Karimi, et al. The latest achievements in plant cellulose-based biomaterials for tissue engineering focusing on skin repair. *Chemosphere*, 2022, 288: 132529. https://doi.org/10.1016/j.chemosphere.2021.132529

[7] S.H. Hamed, E.A. Azooz, E.A.J. Al-Mulla. Nanoparticles-assisted wound healing: A review. *Nano Biomedicine and Engineering*, 2023, 15(4): 425−435. https://doi.org/10.26599/nbe.2023.9290039

[8] Y.N. Zhu, J.M. Zhang, J.Y. Song, et al. A multifunctional pro-healing zwitterionic hydrogel for simultaneous optical monitoring of pH and glucose in diabetic wound treatment. *Advanced Functional Materials*, 2020, 30(6):

1905493. https://doi.org/10.1002/adfm.201905493
[9] Y. Wang, J. Bai. Research progress on the role of microenvironment pH value in chronic wound healing. *Journal of Nursing Science*, 2023, 38: 121–124. (in Chinese)
[10] Z.L. He, J.D. Liu, J. Hu, et al. Facile synthesis of self-healing gels *via* frontal polymerization toward acid–base regulatable wound dressing. *Journal of Materials Science*, 2022, 57(27): 12971−12984. https://doi.org/10.1007/s10853-022-07403-5
[11] T.T. Cui, J.F. Yu, C.F. Wang, et al. Micro-gel ensembles for accelerated healing of chronic wound *via* pH regulation. *Advanced Science*, 2022, 9(22): e2201254. https://doi.org/10.1002/advs.202201254
[12] H. Ehtesabi, S.O. Kalji, L. Movsesian, Smartphone-based wound dressings: A mini-review. *Heliyon*, 2022, 8(7): e09876. https://doi.org/10.1016/j.heliyon.2022.e09876
[13] L.A. Wallace, L. Gwynne, T. Jenkins. Challenges and opportunities of pH in chronic wounds. *Therapeutic Delivery*, 2019, 10(11): 719−735. https://doi.org/10.4155/tde-2019-0066
[14] J. Cheng, Y. Jun, J.H. Qin, et al. Electrospinning versus microfluidic spinning of functional fibers for biomedical applications. *Biomaterials*, 2017, 114: 121−143. https://doi.org/10.1016/j.biomaterials.2016.10.040
[15] Y.Q. Liao. Ben Cao Gang mu. In: Encyclopaedia of the History of Science, Technology, and Medicine in Non-Western Cultures. Selin, H., ed. Dordrecht: Springer Netherlands, 2008: 399–400. https://doi.org/10.1007/978-1-4020-4425-0_8472
[16] Y.P. Liang, J.H. He, B.L. Guo. Functional hydrogels as wound dressing to enhance wound healing. *ACS Nano*, 2021, 15(8): 12687−12722. https://doi.org/10.1021/acsnano.1c04206
[17] L.Y. Qi, K.K. Ou, Y.J. Hou, et al. Unidirectional water-transport antibacterial trilayered nanofiber-based wound dressings induced by hydrophilic-hydrophobic gradient and self-pumping effects. *Materials & Design*, 2021, 201: 109461. https://doi.org/10.1016/j.matdes.2021.109461
[18] C.Y. Liu, W.H. Yao, M. Tian, et al. Mussel-inspired degradable antibacterial polydopamine/silica nanoparticle for rapid hemostasis. *Biomaterials*, 2018, 179: 83−95. https://doi.org/10.1016/j.biomaterials.2018.06.037
[19] Y.Y. Li, J. Zhang, J.P. Yue, et al. Epidermal stem cells in skin wound healing. *Advances in Wound Care*, 2017, 6(9): 297−307. https://doi.org/10.1089/wound.2017.0728
[20] B.C. Dash, Z.Z. Xu, L. Lin, et al. Stem cells and engineered scaffolds for regenerative wound healing. *Bioengineering*, 2018, 5(1): 23. https://doi.org/10.3390/bioengineering5010023
[21] Z.B. Zhou, J.W. Xiao, S.W. Guan, et al. A hydrogen-bonded antibacterial curdlan-tannic acid hydrogel with an antioxidant and hemostatic function for wound healing. *Carbohydrate Polymers*, 2022, 285: 119235. https://doi.org/10.1016/j.carbpol.2022.119235
[22] M.Y. Liu, L. Lin, M.M. Shao, et al. Decellularized human amniotic particles reinforced with GelMA assist wound healing of the oral mucosa *in vivo*. *Materials Express*, 2021, 11(7): 1092–1100. https://doi.org/10.1166/mex.2021.2021
[23] K. Harding, D. Queen. Innovation in wound healing. *International Wound Journal*, 2017, 14(1): 5. https://doi.org/10.1111/iwj.12718
[24] M.N. Nicholas, J. Yeung. Current status and future of skin substitutes for chronic wound healing. *Journal of Cutaneous Medicine and Surgery*, 2017, 21(1): 23−30. https://doi.org/10.1177/1203475416664037
[25] D.C. Hocking, J.R. Brennan, C.H. Raeman. A small chimeric fibronectin fragment accelerates dermal wound repair in diabetic mice. *Advances in Wound Care*, 2016, 5(11): 495−506. https://doi.org/10.1089/wound.2015.0666
[26] J.C. Liu, L. Zhou, F. Wang, et al. Osthole decreases collagen I/III contents and their ratio in TGF-β1-overexpressed mouse cardiac fibroblasts through regulating the TGF-β/Smad signaling pathway. *Chinese Journal of Natural Medicines*, 2018, 16(5): 321−329. https://doi.org/10.1016/S1875-5364(18)30063-3
[27] R.J. Song, X. Mao, S.Q. Tang. κ/β-Carrageenan oligosaccharides promoting polarization of LPS-activated macrophage and their potential in diabetes wound healing. *Materials Science and Engineering: C*, 2021, 121: 111830. https://doi.org/10.1016/j.msec.2020.111830
[28] T.A. Wynn, K.M. Vannella. Macrophages in tissue repair, regeneration, and fibrosis. *Immunity*, 2016, 44(3): 450−462. https://doi.org/10.1016/j.immuni.2016.02.015
[29] A.A. Kalitnik, Y.A. Karetin, A.O. Kravchenko, et al. Influence of carrageenan on cytokine production and cellular activity of mouse peritoneal macrophages and its effect on experimental endotoxemia. *Journal of Biomedical Materials Research Part A*, 2017, 105(5): 1549−1557. https://doi.org/10.1002/jbm.a.36015
[30] M.M. Cui, L.L. Liu, N. Guo, et al. Preparation, cell compatibility and degradability of collagen-modified poly(lactic acid). *Molecules*, 2015, 20(1): 595−607. https://doi.org/10.3390/molecules20010595
[31] F.M. Xiang. Preparation and properties characterization on PLA/OMMT intercalation composites by solution intercalation. *Bulletin of the Chinese Ceramic Society*, 2009, 28: 679–685. (in Chinese)
[32] X. Chai, L. Zhou, C. He. Study on bamboo fiber and sodium alginate enhancing the degradability of polylactic acid. *Acta Materiae Compositae Sinica*, 2023, 40: 3553–3561. (in Chinese) https://doi.org/10.13801/j.cnki.fhclxb.20220901.003
[33] A.E.A. dos Santos, F.V. dos Santos, K.M. Freitas, et al. Cellulose acetate nanofibers loaded with crude annatto extract: Preparation, characterization, and *in vivo* evaluation for potential wound healing applications. *Materials Science and Engineering: C*, 2021, 118: 111322. https://doi.org/10.1016/j.msec.2020.111322
[34] G. Milanesi, B. Vigani, S. Rossi, et al. Chitosan-coated Poly(lactic acid) nanofibres loaded with essential oils for wound healing. *Polymers*, 2021, 13(16): 2582. https://doi.org/10.3390/polym13162582
[35] Y. Chen, H. Yue, R. Zhu, et al. Research progress of electrospinning antibacterial materials. *New Chemical Materials*, 2023, 51(3): 79–83. (in Chinese) https://doi.org/10.19817/j.cnki.issn1006-3536.2023.03.014
[36] Y. Wu, Q. Zhong, Y. Xing, et al. Research progress of electrospinning nanofiber membranes in air filtration. *Fine Chemicals*, 2021, 38: 153–1541. (in Chinese)
[37] S. Wang, Q.B. Han, D.J. Zhang, et al. Development and characterization of carboxymethyl chitosan/sodium alginate/gelatin methacryloyl hydrogels as wound dressing materials. *Materials Express*, 2022, 12(12): 1572−1576. https://doi.org/10.1166/mex.2022.2301
[38] G. Singh, A. Chanda. Mechanical properties of whole-body soft human tissues: A review. *Biomedical Materials*, 2021, 16(6): 062004. https://doi.org/10.1088/1748-605x/ac2b7a
[39] M. Davoudabadi, S. Fahimirad, A.L. Ganji, et al. Wound

healing and antibacterial capability of electrospun polyurethane nanofibers incorporating *Calendula officinalis* and *Propolis* extracts. *Journal of Biomaterials Science, Polymer Edition*, 2023, 34(11): 1491−1516. https://doi.org/10.1080/09205063.2023.2170138

[40] A. Gul, I. Gallus, A. Tegginamath, et al. Electrospun antibacterial nanomaterials for wound dressings applications. *Membranes*, 2021, 11(12): 908. https://doi.org/10.3390/membranes11120908

[41] C. Merzougui, F.Y. Miao, Z.M. Liao, et al. Electrospun nanofibers with antibacterial properties for wound dressings. *Journal of Biomaterials Science Polymer Edition*, 2022, 33(16): 2165−2183. https://doi.org/10.1080/09205063.2022.2099662

[42] S.W. Sun, M.Q. Hao, C.B. Ding, et al. SF/PVP nanofiber wound dressings loaded with phlorizin: Preparation, characterization, *in vivo* and *in vitro* evaluation. *Colloids and Surfaces B: Biointerfaces*, 2022, 217: 112692. https://doi.org/10.1016/j.colsurfb.2022.112692